Developments in realistic design for aperiodic Mo/Si multilayer mirrors

A.L. Aquila, F. Salmassi, F. Dollar, Y. Liu, and E.M. Gullikson
Center for X-Ray Optics, Lawrence Berkeley National Lab 2-400, Berkeley, CA 94720

Abstract: Aperiodic multilayers have been designed for various applications, using numeric algorithms and analytical solutions, for many years with varying levels of success. This work developed a more realistic model for simulating aperiodic Mo/Si multilayers to be used in these algorithms by including the formation of $MoSi_2$. Using a genetic computer code we were able to optimize a 45° multilayer for a large bandpass reflection multilayer that gave good agreement with the model.

I. Introduction

Aperiodic multilayer structures have been developed [1,2] for various applications that require larger wavelength/energy bandpasses than can be achieved with periodic structures. These structures have been used with great success under the title of "supermirrors" in both neutron optics, and grazing incidence hard x-ray optics. However, the use of aperiodic multilayers in large angle soft x-ray/extreme ultraviolet (EUV) optics has been hampered due to lack of agreement in the optimizing simulations compared to the deposited thin film optics. Often the measured reflectivity can differ significantly from the design goal. While these differences could result from inaccuracies in the deposition process there is also the predictable error caused by the intermixing at the multilayer interfaces. The motivation of this work is to demonstrate improvements in the simulation of aperiodic multilayers to allow for there use in applications such as bandpass filters, and integrated reflectivity mirrors.

The Mo/Si multilayer system is probably the best studied system due to its importance as a high reflectance coating for EUV lithography and astronomy. This paper demonstrates for the Mo/Si system that when the formation of $MoSi_2$ is properly included in the design of an aperiodic multilayer structure, it is possible to fabricate a multilayer with a performance very close to the design. The silicide simulation process is discussed in Section 2. Section 3 discusses the computational optimization process and section 4 describes the sample preparation and compares the designed and measured reflectivity.

II. Silicide

It is well known that the intertermixing of the Mo and Si plays an important role in determining the structure of a Mo/Si multilayer. The multilayer not

only becomes a three-component system but also contracts as the Mo and Si are consumed in the interface layer changing the multilayer period. This is illustrated in Fig. 1 for an aperiodic structure where the left most image is what would be expected without considering the intermixing and the center image is the expected structure when intermixing is taken into account as described below. The right image is a TEM of the fabricated multilayer.

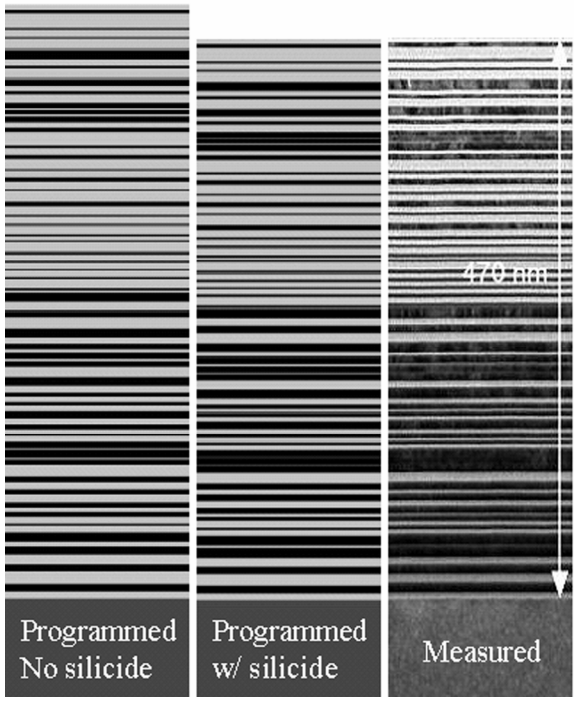

Fig. 1. Simulation of the programmed Mo and Si thickness (Left); modeling the contraction caused by MoSi2 formation (Center); actual TEM cross-section of the fabricated multilayer (Right). This demonstrates that including the silicide formation is required to match the simulation to the actual sputtered sample.

The interdiffused silicide regions in standard Mo/Si multilayers have been observed to be asymmetric with the silicide layer being thicker for the Mo deposited on Si interface than for the Si deposited on Mo interface. Measurements [3] indicate that inter-diffused layer is amorphous with a stochiometry of nearly $MoSi_2$. An amorphous to crystalline transition occurs in the Mo layer for a thickness around 2 nm. This transition results in a significant decrease in the silicide layer for the Si on Mo interface [4].
In our modeling it is assumed that the interface layers are $MoSi_2$. For the Mo on Si interface the silicide layer thickness increases to ~0.95 nm as the Mo is deposited [3]. For Si on Mo the silicide layer is assumed to be ~0.95 nm when the deposited Mo layer is thinner than the critical thickness of 2.0 nm and ~0.6 nm if the deposited Mo thickness is greater than 2.0 nm. For each

nanometer of $MoSi_2$ that is formed it takes 1nm of Si and .39 nm of Mo resulting in a contraction of 39% of the silicide layer thickness. This contraction reduces the overall thickness of the multilayer stack changing the d spacing of each layer and thus its wavelength dependent reflectivity. It is noted that the interfaces composition and thickness will vary between different deposition methods; we choose interdiffusion parameters based on measurements conducted, and published in the literature, on nearly identical deposition methods to insure the realism of the simulation.

III. Optimization process

The multilayer mirrors were optimized using a single parent, mutation based, genetic algorithm [5] also called a Luus-Jaakola algorithm [6]. It is noted that this method does not guarantee the absolute global optimization, is slower than many other algorithms, and is also dependent on the initial seed multilayer or starting condition. The algorithm was chosen for its simplicity, ease of coding and its ability to be run in parallel unlike simulated annealing algorithms. With computational time being relatively inexpensive, the speed of the algorithm is less of a critical factor compared to the results produced by the optimization. With a genetic algorithm a global optimization can be reached with this algorithm if an optimal seed is used.

The process takes a seed or parent multilayer composing of a stack of Mo/Si pairs; each Mo or Si layer is considered a gene. For our specific samples a 60 or 40 bi-layer stack of Mo/Si was used. The 60 bi-layer pair was initially chosen to ensure that we obtained an optically thick mirror, however it soon became apparent that we could remove the bottom 10 to 20 layers without significantly affecting the reflectivity. This made a organism composed of 120, or 80, ordered genes with each gene being a number representing the thickness of the layer in multilayer and the gene number representing the position of the layer in the stack. The current seed multilayer is a standard periodic Mo/Si stack, this is a non-optimized seed multilayer for large bandpasses. Using a pre-developed analytic solution [7] can create optimal seed multilayers, however current analytic solutions have only been developed for two component systems. Simulating the growth of $MoSi_2$ and the contraction of the multilayer in these solutions diminishes its usability.

Small Gaussian random thickness variations, or mutations, were added or subtracted from each gene in the parent's multilayer stack. With the exception that we set a lower bound on the thickness of any layer to 1 nm. These new variations formed the children of the parent multilayer. In this specific optimization 100's of children were used due to the large number of genes. To put it another way we are considering points in and on a sphere centered at the parent with radius the size of the thickness variation in 120 dimensional space. We then simulated the effects of $MoSi_2$ and the contraction of the multilayer and roughness between each layer of the child multilayer. Each of

the children are evaluated for reflectivity using standard methods [8] and given a numerical ranking. A merit function process chooses the numerical ranking where the wavelength dependent reflectivity was compared against a desired function:

$$M = \int \left(R_m - R_c\right)^2 d\lambda \qquad (1)$$

Where R_m is the merit function or desired reflectivity curve, R_c is the simulated child's multilayer reflectivity curve, and M is the minimization parameter or numerical ranking. The child with the smallest M became the new parent for the next generation.

This generational process is repeated until all the children of the parent multilayer have larger values of M than the parent. This occurs when the multilayer parameters have drifted to a minimum. Then the size of the mutations is reduced, and more generations are simulated. This process stops when the size of the mutations is reduced to a value below the coating tolerance of our deposition machine. At this point we have an optimized reflectivity coating.

When looking at solutions developed using genetic algorithms it is often difficult to determine why the solution is an optimization or if the optimization is a global optimization. No only using different starting conditions could possibly obtain different optimizations; also due to the fact that the children are based on random mutations if an insufficient number of children is used then different local optimizations can be achieved with the same starting conditions. Looking at fig. 1 the bottom half of the multilayer looks intuitively incorrect due to the larger thickness of Mo layers that act as absorbers. After conducting simulations with the bottom layers removed it became clear that only the top 80 to 100 layers play a role in the simulation the rest of the layers would be below the attenuation length and have not effect. Also the sharp edge bandpass structure develops in the top 40 layers consisting of three large peaks with large fluctuation. The remaining layers acting to flatten out the top of the structure.

IV. Sample preparation and reflectivity measurements

The multilayers were deposited using a DC magnetron sputtering system. The system has a base pressure of better than $1x10^{-7}$ torr. The sputtering was performed with Ar gas at a pressure of 1 mtorr. The target powers were 50 W for Mo and 100 W for Si resulting in an average deposition rate of 0.59 nm/sec for Mo and 0.83 nm/sec for Si. The mirror substrate is moved over the sputter guns at a velocity, which depends on the desired layer thickness. The absolute sputtering rates were measured using both an alpha-step tool and reflectometry on periodic multilayer coatings. By changing the velocity of the sample for each target we are able to control the thickness of the layer to within 1% of the desired thickness.

The reflection measurements of the bandpass multilayers were preformed at ALS calibration and standards beamline 6.3.2 [9]. This beamline is designed for absolute reflectivity measurements in the EUV and soft x-ray regions and is routinely used in multilayer EUV reflectometry measurements. The beamline has high spectral purity, and a spectral resolving power ($\lambda/\Delta\lambda$) of up to 7000, a wavelength accuracy of 10^{-3} nm, and a reflectivity accuracy of 0.1% (absolute). These characteristics make it ideal for testing multilayer mirrors. In order to demonstrate the importance of the silicide formation two 45-degree mirrors were designed, one that included the silicide interface layers and the other, which did not. Both mirrors were designed with the same output goal parameters (R_m): a bandwidth of 3 nm centered at 14.25 nm with an average reflectivity of 20% within the bandpass and 0% reflectivity outside this bandpass.

The results for the multilayer which was designed without taking the silicide layers into account is shown in Fig. 2. This mirror consisted of 80 layers with a Si topmost layer to limit oxidation. The dashed curve is the optimized reflectivity resulting from the genetic algorithm. The measured reflectivity (points) is much less uniform than the expected from the design and is shifted to shorter wavelengths as would be expected due to contraction. The solid curve in Fig. 2 is calculated by including the silicide layers in the modeled structure and is in very good agreement with the measured reflectivity. The main area of disagreement is near the Si L edge at 12.4 nm and could be a result of inaccuracy of the $MoSi_2$ optical constants.

Figure 3 shows the results for a broadband mirror that incorporated silicide in its optimization This mirror was composed of 100 layers with Si being the topmost layer to limit oxidation. The structure of this multilayer is shown in Fig. 1. Note the good agreement of the measurements with the simulated structure in Fig. 1 and with the design reflectivity in Fig. 3. The agreement is not exact, and as the TEM image shows there are slight discrepancies in the thickness profile (Fig. 1) due to our sputtering system. We believe this accounts for the discrepancies in reflectivity and the slight wavelength shift.

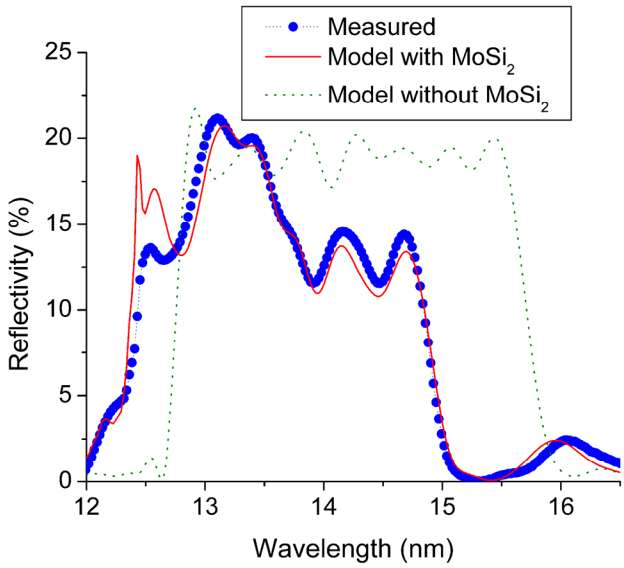

Fig. 2. This graph shows an optimization for a 45-degree Mo/Si mirror that did not include $MoSi_2$ formation (dashed black curve) and the same multilayer stack with silicide formation (solid red curve). We deposited this mirror and measured it (blue curve). Notice the good agreement to the model that included silicide.

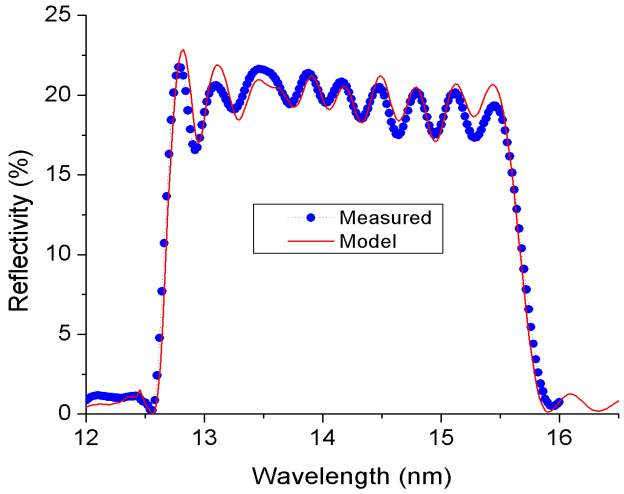

Fig. 3. This graph shows the reflectivity for the mirror and the model with $MoSi_2$ is considered. The mirror is a 45 degree mirror with a 3 nm bandwidth. A cross-section TEM image of this mirror is shown in Fig. 1.

When creating aperiodic multilayers attention to the exact sputtering rates is critical. For a typical periodic multilayer mirror a 1% error in the sputtering rate of one of the materials shifts the wavelength of the reflectivity curve by a

factor of γ*1% or (1-γ)*1%. Where γ is the ratio of Mo thickness to total thickness. For an aperiodic multilayer an error in the deposition rate of one of the materials not only shifts the reflectivity curve but will also change the shape. Furthermore, if we consider a layer of Mo in a aperiodic multilayer that is close to the critical thickness then a shift in sputtering rates could change which side of the critical thickness the layer is on changing the $MoSi_2$ thickness by 15% and a 7% change in Mo thickness. In an aperiodic multilayer these changes will not only shift the reflectivity curve but also change the shape of the reflectivity curve because these changes only will occur in a few layers. If the simulation is to be realistic, care must be take to insure that the Mo thickness for each layer determined by the optimization is further from 2 nm then the thickness error of the sputtering system.

V. Conclusion

We have demonstrated the need to include interdiffusion in the development and optimization of aperiodic Mo/Si multilayer structures. This was demonstrated with an EUV broadband mirror designed for 45 degrees incidence. By modeling silicide formation in the optimization process it is possible to design and fabricate multilayer mirrors with reflectance close to the design goal.

Acknowledgment

This work was supported by the National Science Foundation Engineering Research Center for Extreme Ultraviolet Science and Technology and the US Department of Energy.

References

1. Z. Wang and A. G. Michette, "Broadband multilayer mirrors for optimum use of soft x-ray source output," J. Opt. A: Pure Appl. Opt. **2,** 452–457 (2000).

2. S. Yulin, T. Kuhlmann, T. Feigl, and N. Kaiser, "Spectral reflectance tuning of EUV mirrors for metrology applications," in *Emerging Lithographic Technologies VII*, R.L. Engelstad ed., Proc. SPIE **5037,** 286-293 (2003).

3. S. Bajt, D. Stearns, and P. Kearney, "Investigation of the amorphous-to-crystalline transition in Mo/Si multilayers," J. Appl. Phys. **90**, 1017-1025 (2001).

4. R.S. Rosen, D. G. Stearns, M. A. Viliardos, M. E. Kassner, S. P. Vernon, and Y. Cheng. "Silicide layer growth rates in Mo/Si multilayers," Appl. Opt. **32**, 6975-6980 (1993).

5. Similar to work done by: P. D. Binda, and F. E. Zocchi, "Genetic algorithm optimization of X-ray multilayer coatings," in *Advances in Computational Methods for X-Ray and Neutron Optics*, M. Sanchez del Rio ed., Proc. SPIE **5536***,* 97-108 (2004).

6. B. Liao and R. Luus, "Comparison of the Luus-Jaakola optimization procedure and the genetic algorithm," Engineering Optimization **37**, 381-398 (2005)

7. V. Kozhevnikov, I. N. Bukreeva, and E. Ziegler, "Design of X-ray supermirrors," Nuclear Instruments and Methods in Physics Research A **460**, 424-443 (2001).

8. E. Spiller, "Interference in thin films: theory," in *Soft X-ray Optics* (SPIE Optical Engineering Press, 1994), pp. 101-107.

9. E. M. Gullikson, S. Mrowka, and B. B. Kaufmann, "Recent developments in EUV reflectometry at the Advanced Light Source," in *Emerging Lithographic Technologies V*, E. A. Dobisz ed., Proc. SPIE **4343**, 363 (2001).